Pulse properties of external-cavity mode-locked semiconductor lasers

Josep Mulet[1,2], **Marcel Kroh**[3], **Jesper Mørk**[2]

[1]*Institut Mediterrani d'Estudis Avançats - IMEDEA (CSIC-UIB), Ed. Mateu Orfila, Campus Universitat de les Illes Balears, E-07122 Palma de Mallorca, Spain.*
[2]*Research Center COM, NanoDTU, Technical University of Denmark, Building 345V, DK-2800 Kgs. Lyngby, Denmark.*
[3]*Heinrich-Hertz-Institut für Nachrichtentechnik Berlin GmbH, Einsteinufer 37, D-10587 Berlin, Germany.*
mulet@imedea.uib.es

Abstract: The performance of an external-cavity mode-locked semiconductor laser is investigated both theoretically and experimentally. The optimization analysis focuses on the regimes of stable mode locking and the generation of sub-picosecond optical pulses. We demonstrate stable output pulses down to one picosecond duration with more than 30 dB trailing pulse suppression. The limiting factors to the device performance are investigated on the basis of a fully-distributed time-domain model. We find that ultrafast gain dynamics effectively reduce the pulse-shaping strength and inhibit the generation of femtosecond optical pulses.

OCIS codes: (140.4050) Mode-locked lasers, (140.5960) Semiconductor lasers

References and links

1. H. Yokoyama, "Highly reliable mode-locked semiconductor lasers," IEICE Trans. Electron. **E85-C**, 27–36 (2002).
2. P. J. Delfyett, L. T. Florez, N. Stoffel, T. Gmitter, N. C. Andreadakis, Y. Silberberg, J. P. Heritage, and G. A. Alphonse, "High-power ultrafast laser diodes," IEEE J. Quantum Electron. **10**, 2203–2219 (1992).
3. S. Bischoff, M. P. Sørensen, J. Mørk, S. D. Brorson, T. Franck, J. M. Nielsen, and A. Møller-Larsen, "Pulse-shaping mechanism in colliding-pulse mode-locked laser diodes," Appl. Phys. Lett. **67**, 3877–3879 (1995).
4. S. Gee, G. A. Alphonse, J. C. Connolly, C. Barty, and P. J. Delfyett, "Ultrashort pulse generation by intracavity spectral shaping and phase compensation of external-cavity modelocked semiconductor lasers," IEEE J. Quantum Electron. **36**, 1035–1040 (2000).
5. R. Ludwig, S. Diez, E. Ehrhardt, L. Küller, W. Pieper, and H. G. Weber, "A tunable femtosecond modelocked semiconductor laser for applications in OTDM-systems," IEICE Trans. **E81-C**, 140–145 (1998). And references therein.
6. J. L. A. Dubbeldam, J. A. Leegwater, and D. Lenstra, "Theory of mode-locked semiconductor lasers with finite absorber relaxation times," Appl. Phys. Lett. **70**, 1938–1940 (1997).
7. G. P. Agrawal and N. A. Olsson, "Self-phase modulation and spectral broadening of optical pulses in semiconductor laser amplifiers," IEEE J. Quantum Electron. **25**, 2297–2306 (1989).
8. A. Uskov, J. Mørk, and J. Mark, "Theory of short-pulse gain saturation in semiconductor laser amplifiers," IEEE Photon. Technol. Lett. **4**, 443–446 (1992).
9. J. Mulet and J. Mørk, "Analysis of timing jitter in external-cavity mode-locked semiconductor lasers," IEEE J. Quantum Electron. **42**, no. 3, March (2006).
10. C. Harder and K. Y. Lau and A. Yariv, "Bistability and pulsations in semiconductor lasers with inhomogeneous current injection," IEEE J. Quantum Electron. **18**, 1351-1361 (1982).
11. J. Paslaski and K. Y. Lau, "Parameter ranges for ultrahigh frequency mode locking of semiconductor lasers," Appl. Phys. Lett. **59**, 7–9 (1991).
12. M. Schell, M. Tsuchiya, and T. Kamiya, "Chirp and stability of mode-locked semiconductor lasers," IEEE J. Quantum Electron. **32**, 1180–1190 (1996).

#10095 - $15.00 USD Received 22 December 2005; revised 30 January 2006; accepted 31 January 2006

13. H. A. Haus and A. Mecozzi, "Noise of mode-locked lasers," IEEE J. Quantum Electron. **29**, 983–996 (1993).
14. Y. K. Chen, M. C. Wu, T. Tanbun-Ek, R. A. Logan, and M. A. Chin, "Subpicosecond monolithic colliding-pulse mode-locked multiple quantum well lasers," Appl. Phys. Lett. **58**, 1253–1255 (1991).

1. Introduction

Mode-locked semiconductor lasers are optical sources of picosecond pulses for several applications including: high-speed optical time-division multiplexed (OTDM) communication systems, optical clocking and sampling, etc. The maximum attainable bitrate in these systems is determined by the shortest temporal width and timing jitter of the pulses; hence, a thorough understanding of the underlying mechanisms is of crucial interest for future applications. In spite of the limited integrability of external-cavity mode-locked semiconductor lasers (ECMLLs), they are particularly interesting as optical sources for laboratory use, tunable both in wavelength and repetition rate [1] and for high power generation [2]. To date, most of the mode-locked semiconductor lasers generating pulses shorter than one picosecond are of the type of colliding-pulse mode-locking which are not tunable [3]. In ECMLLs, two different approaches have been devised to overcome the picosecond frontier: i) hybrid mode-locking with intracavity dispersion compensation [4] and ii) integrated ion bombarded saturable absorbers [5]. However, these systems are characterized by either an extensive set-up or require an absorber technology which is expensive and does not allow for any external control. Hence, in practice, sub-ps pulse generation in multi-GHz mode-locked lasers based on reverse-biased absorbers generally requires external manipulation of the pulses, such as pulse compression stages. Moreover, ECMLLs display a number of detrimental effects that require special attention before they can be useful for practical applications. These effects include the appearance of trailing pulses, regimes of incomplete mode-locking, onset of self-pulsation, etc.

The pulsewidth in a mode-locked laser is determined by the balance between pulse shortening and broadening (due to dispersion). For a slow absorber, pulse shortening is effective when the saturable absorber (ABS) is more easily saturated than the semiconductor optical amplifier (SOA). The nonlinear saturation processes in SOA (ABS) effectively sharpen the trailing (leading) edge of the pulse, thus producing pulse compression. For finite absorber relaxation times, the relative contribution of SOA is less important and the shortening is primarily due to the absorber [6]. These arguments, however, neglect the contribution from ultrafast gain dynamics. The saturation energy of SOA and ABS, determining the pulse shaping strength, have contributions from gain depletion (differential saturation) [7] and non-equilibrium processes [8]. Ultrafast processes are increasingly important when the pulsewidth reaches their characteristic sub-picosecond time scales, specially due to hot carrier thermalization [2]. Since ultrafast effects modify the saturation energies and, in turn, the shortening strength, they ultimately define the shortest attainable pulsewidth. In this paper, we experimentally and theoretically investigate the pulse properties of a multiple quantum well (MQW) buried heterostructure ECMLL. A fully-distributed time-domain model is validated with experimental characterization results. The interplay of different physical mechanisms is discussed in the paper. Finally, the model is used to analyze the factors limiting the shortest pulsewidth.

2. Laser setup and model

The mode-locked laser used in the experiments is a two section six-QW buried heterostructure plus an external cavity. A 560 μm-long section is forward biased to provide optical gain, thus acting as an SOA. The saturable absorption is achieved by reverse biasing a 50 μm-long section. A separation of 20 μm between both sections ensures electrical isolation ($R \sim 2$ kΩ). The absorber facet has the reflectivity of a semiconductor-air interface and is used as output to a fiber taper. The absorber is placed in a self-colliding position, i.e., the leading and trailing parts of

#10095 - $15.00 USD Received 22 December 2005; revised 30 January 2006; accepted 31 January 2006

the pulse encounter due to reflection at the absorber facet. The other laser facet is antireflection (AR) coated, with residual reflectivity $R_{AR} \sim 10^{-4}$, and coupled to the external cavity. Hence, the laser diode cannot lase by itself unless receives feedback from a diffraction grating. A GRIN rod lens is used to collimate the optical mode in the external cavity. Fine tuning of the diffraction grating allows us to adjust the repetition rate to 10 GHz and the emission wavelength to 1.55 μm. The pulsewidth is obtained from second-harmonic autocorrelation techniques and deconvolved assuming an hyperbolic secant pulse shape. The spectral width of the pulses is obtained from an optical spectrum analyzer. Finally, amplitude and timing jitter are measured using an electrical spectrum analyzer.

A fully-distributed time-domain model, detailed in Ref. [9], is implemented to describe the mode-locking dynamics. The ECMLL simulator includes the nonlinear and ultrafast dynamics of gain/absorption, dispersion, self-phase modulation and spontaneous emission noise. The optical propagation is described by traveling-wave equations which are numerically solved within the multi-section laser diode using a finite differences scheme. Appropriate boundary conditions for two counter-propagating waves naturally account for multiple reflections within the diode chip and external cavity. The external cavity is effectively described through a delayed feedback term, which is spectrally filtered by the diffraction grating. The SOA and absorber models describe, in the relaxation rate approximation, deviations from quasi-equilibrium Fermi-Dirac distributions due to spectral-hole burning (SHB) and carrier heating (CH). An effective rate equation model [8] describes the depletion in local carrier density, resonant with the lasing transition, due to SHB and the energetic redistribution of electrons and holes due to CH. In the absorber, the nonlinear dependence of the absorption recovery time with the reverse voltage due to carrier sweep-out is phenomenologically described and it amounts to $\tau_{abs} \gtrsim 10$ ps for $V_{abs} \approx -2$ V. Furthermore, bandgap renormalization due to the quantum-confined Stark effect leads to red-shift of the absorption edge, which allows us, in a simple way, to map the unsaturated absorption level into applied reverse voltage. However, the effects of the driving circuitry on the absorber characteristics have not been included [10]. The parameters in the model (See [9]) are taken according to the experimental conditions and validated by the results presented in the next section.

3. Results

We first describe the different operation regimes that appear upon simultaneous variation of the reverse voltage in the absorber and the injection current to SOA [Fig. 1(a)]. We start the investigation with a diffraction grating of 300 lines/mm yielding an optical bandwidth of ~ 8 nm. The other external cavity parameters have been adjusted to minimize the threshold current and to tune the emission wavelength with respect to the gain peak. Mode-locking starts almost immediately once the injection current exceeds the laser threshold which increases with reverse bias due to higher unsaturated absorption. Light-current characteristics display light-jumps for reverse voltages below -1 V, and hysteresis cycles have been observed for certain values below -2 V. These behaviors have been explained as an interplay between the laser, the absorber and the external driving circuitry for the absorber [10]. The operation is free of self-pulsation at 10 GHz repetition rate [11]. In order to inhibit the Q-switching instability, the design provides low cavity losses, moderate contrast in saturation energies between SOA and ABS, and fast recombination time in SOA. The shaded regions in Fig. 1(a) provide the driving conditions for stable and low amplitude noise mode-locking. The regime of stable mode-locking extends over a wider current interval for large reverse bias in the absorber. For injection currents beyond this interval, mode-locking reaches an unstable regime characterized by a substantial increase in amplitude noise. At this point, a coherence spike on top of the autocorrelation function can be identified. In simulations, the onset of incomplete mode-locking (IML) manifests itself as

#10095 - $15.00 USD Received 22 December 2005; revised 30 January 2006; accepted 31 January 2006

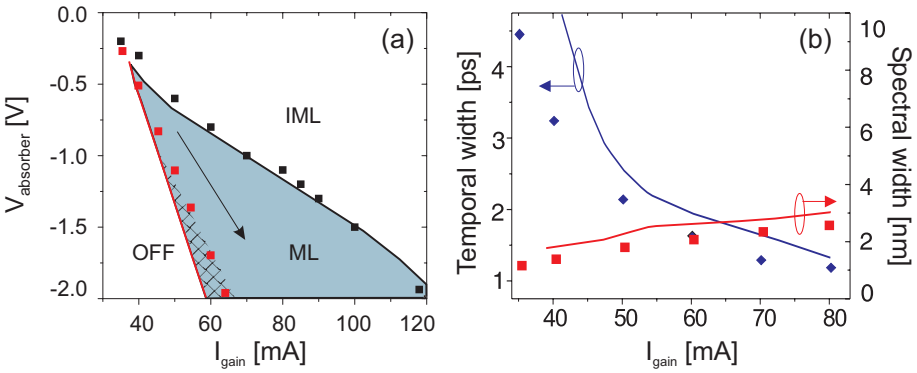

Fig. 1. (a) Regimes of operation: No laser emission (OFF), stable mode-locking (ML), incomplete mode-locking (IML), and appearance of light-jumps in the light-current characteristics (dashed region). (b) Evolution of the temporal and spectral width of the pulses. Experiments (symbols) and simulations (solid lines).

a slow irregular envelope of the pulse train. Numerical simulations show that this instability occurs even for perfect AR coatings. The reason is different: for sufficiently large gain, fluctuations of the background can grow at the leading edge of the pulse yielding a dynamical substructure of the pulse. Furthermore, the position of the IML boundary depends on the chirp of the pulses, cavity dispersion and bandwidth [12]. Thus, moderate self-phase modulation, accomplished with low Henry alpha-factors, can effectively shift the IML boundary to higher injection currents. The numerically obtained regions in Fig. 1(a) show good agreement with the experimental results over the explored parameter range.

Next, we look for the optimum driving conditions yielding the shortest pulsewidth. Figure 1(b) shows the dependence of the temporal and spectral FWHM of the pulses. The data are obtained when moving along the arrow in Fig. 1(a). The pulses shorten with the reverse bias, whereas the spectral width increases almost linearly. The optimum operation point is found for large reverse bias and currents close-to-threshold as found in Ref. [11]. At the optimum point, the pulse shape closely matches a sech^2 function and pulses are nearly transform limited ($\Delta t\,\Delta\nu \approx 0.35$). However, we find weak trailing pulses due to internal reflections at the imperfect AR facet. The trailing pulses can be suppressed down to ~ 30 dB for the largest reverse bias accessible. For higher injection levels to SOA, we find that the pulses broaden due to additional self-phase modulation and the time-bandwidth product increases. Pulse shortening by reverse biasing relies on three combined effects: the faster recovery of the absorption, the enhanced contrast in saturation energies between SOA and absorber and the partial compensation of self-phase modulation accrued in SOA and absorber. Experimental and numerical dependencies show a good agreement over a wide parameter range.

In order to analyze the performance of the ECMLL as an ultrashort pulse source, we investigate the dependence of the pulsewidth with the diffraction grating bandwidth ($\Delta\lambda_G$). Experimentally, the optical bandwidth is varied by using different diffraction gratings with resolution ranging from 150 to 1200 lines/mm. As a general trend, the larger the bandwidth, the narrower the stable region for mode-locking due to the earlier appearance of IML [12]. Figure 2 (a) shows that the shortest temporal width of the stable pulses reduces when increasing the optical bandwidth. The shortening is noticeable for $\Delta\lambda_G < 5$ nm, where the pulses are limited by the grating bandwidth and are almost transform limited. In this regime, the spectral width of the pulses increases linearly with the grating bandwidth. For $\Delta\lambda_G > 10$ nm, however, the pulsewidth shortens little and the spectral width increases sub-linearly, meaning that the

#10095 - $15.00 USD Received 22 December 2005; revised 30 January 2006; accepted 31 January 2006

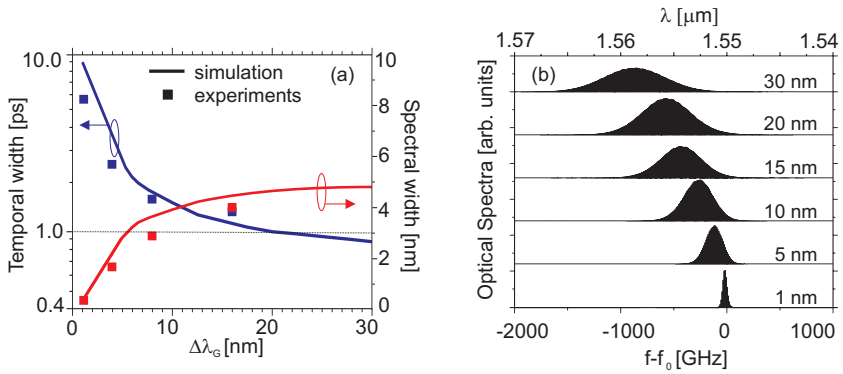

Fig. 2. (a) Temporal and spectral width of the pulses versus the grating bandwidth. Simulations shown as solid lines and symbols are measurements. (b) Simulated frequency combs for different grating bandwidths.

pulses do not cover the entire available optical bandwidth. This predicted scenario is in good agreement with the experimental data shown in Fig. 2 (a). Numerical simulations of the present device show that the temporal width of the stable pulses can be reduced down to one picosecond when the bandwidth of the grating is increased up to $\Delta\lambda_G = 30$ nm. This effect is accompanied by a spectral broadening as shown in the optical spectra of Fig. 2(b). In contrast to narrow bandwidths, where we found nearly transform limited pulses, the time-bandwidth product increases with $\Delta\lambda_G$ indicating that the pulses accumulate chirp, which, in turn, affect their stability. Two additional points are worth mentioning. First, in order to avoid excessive timing jitter associated with ASE and Gordon-Haus noise [13], operation of the ECMLL below the characteristic bandwidth ($\Delta\lambda_G \lesssim 10$ nm) is recommended. In this regime, integration of the phase-noise spectrum between 100 Hz-10 MHz provides ~ 70 fs of timing jitter when 20 dBm RF-power is applied to the absorber section. Second, the fact that the spectral width of the pulses is narrower than the available spectrum indicates that they are not bandwidth limited and nonlinear saturation processes play a leading role. The latter will be analyzed in detail with the aid of numerical simulations.

Thus far, the ECMLL simulator has been validated with the experimental results. In order to clarify the mechanisms limiting the shortest pulsewidth and the appearance of a characteristic optical bandwidth, the simulations have been repeated, artificially turning-off the contributions from ultrafast gain dynamics, i.e., assuming quasi-equilibrium carrier distributions. As a consequence, the pulsewidth, indicated by diamond symbols in Fig. 3(a), is significantly shorter than in the presence of ultrafast effects for those pulses not limited by the optical bandwidth. In order to better understand this effect, the 3 dB saturation energy of SOA and absorber have been separately determined for the same operation conditions as in the mode-locked laser. The ratio of saturation energies $s \equiv E_{sat}^{SOA}/E_{sat}^{ABS}$ is plotted in Fig. 3(b) versus the pulsewidth of an injected hyperbolic-secant pulse for different thermalization times of hot carriers. For pulses below one picosecond, which roughly corresponds to the carrier thermalization time scale, the saturation energy of SOA and absorber depends on the pulsewidth due to ultrafast gain dynamics. Moreover, in the absorber, it depends on its length since the self-colliding effect helps to bleach the absorption more efficiently [14]. In the absence of ultrafast effects E_{sat}^{SOA} is constant. Hence, the dashed line in Fig. 3(b) shows that the s parameter is proportional to $1/E_{sat}^{ABS}$ which is solely determined by the self-colliding mechanism. In this case, the curve indicates that the maximum bleaching efficiency of the absorber occurs at an input pulsewidth of 350 fs. When ultrafast effects come into play, the saturation energy of SOA monotonically decreases

#10095 - $15.00 USD Received 22 December 2005; revised 30 January 2006; accepted 31 January 2006

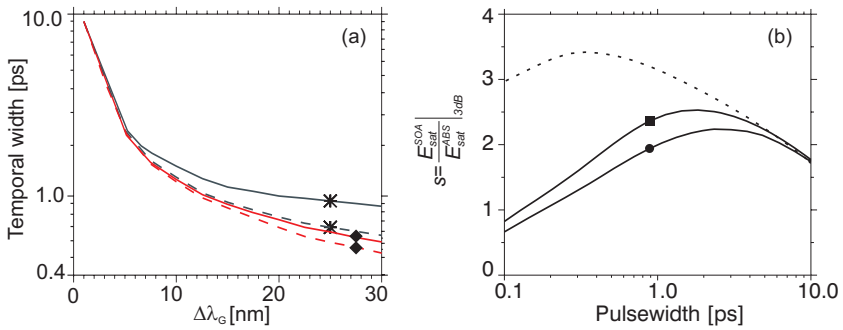

Fig. 3. Contributions to the pulsewidth. (a) Uncompressed pulsewidth shown by solid lines and after linear chirp removal by dashed lines. Simulations are done including ($*$) and artificially turning-off ultrafast effects (⧫). (b) Ratio of 3dB saturation energies between SOA and absorber without (dashed) and including (solid) ultrafast effects: the thermalization time for carriers is 1 ps (■) and 5 ps (●).

with the pulsewidth [8]. When combining the saturation effects of the ABS and SOA, there is a substantial reduction in *s*-parameter for pulsewidths shorter than one picosecond. Furthermore, the reduction in *s*-parameter is more noticeable for large thermalization times of carriers. As already discussed in the introduction, the effective pulse shortening in a mode-locked laser with slow saturable absorber relies on values of *s* much larger than one. Therefore, these results qualitatively explain the change in tendency for the pulsewidth around 1 ps observed in Fig. 3(a), that corresponds to a maximum in *s*-parameter in Fig. 3(b). Besides the modification in effective pulse shaping strength, pulse chirp significantly increases for wide bandwidths, and the time-bandwidth product increases with $\Delta\lambda_G$. In order to evaluate the relative influence of this effect, the linear part of the chirp is removed by numerically propagating the output pulses in a proper length of normal dispersion fiber. Numerical simulations, shown in dashed lines in Fig. 3(a), demonstrate that stable pulses as short as $\sim$ 500 fs can be generated, however, at the expense of including an external pulse compression stage.

4. Conclusions

The mode-locking performance of an external-cavity multi-quantum well buried-heterostructure diode laser has been experimentally characterized and analyzed on the basis of a comprehensive fully-distributed time-domain model. The optimum driving conditions that allow for good trailing pulse suppression, short and nearly-transform limited optical pulses, and moderate timing jitter levels occur when the laser is driven near the mode-locking threshold and for large reverse bias. We have investigated the possibility of sub-ps pulses by increasing the optical bandwidth. Beyond an optimum grating bandwidth, we find a distinctive trade-off between pulsewidth, mode-locking stability and timing jitter. In this regime, ultrafast gain dynamics inhibit the generation of shorter optical pulses due to the weaker pulse shaping strength, mainly caused by the reduced saturation energy of the amplifier.

Acknowledgments

The authors gratefully acknowledge funding from the EU project TOPRATE IST-2000-28657. J. Mulet is also supported by the Spanish CSIC through the program I3P-PC2003 and by the MEC through the project CONOCE-2: FIS2004-00953.

#10095 - $15.00 USD Received 22 December 2005; revised 30 January 2006; accepted 31 January 2006